

## miR-497 suppresses cycle progression through an axis involving CDK6 in ALK-positive cells

Coralie Hoareau-Aveilla,<sup>1,2,3\*</sup> Cathy Quelen,<sup>1,2,3\*</sup> Annabelle Congras,<sup>1,2,3#§</sup> Nina Caillet,<sup>1,2,3#§</sup> Delphine Labourdette,<sup>4</sup> Christine Dozier,<sup>1,2,3</sup> Pierre Brousset,<sup>1,2,3,5,6,7§</sup> Laurence Lamant<sup>1,2,3,5,6,7§</sup> and Fabienne Meggetto<sup>1,2,3,5,6,7§</sup>

<sup>1</sup>Inserm, UMR1037 CRCT, F-31000 Toulouse, France; <sup>2</sup>Université Toulouse III-Paul Sabatier, UMR1037 CRCT, F-31000 Toulouse, France; <sup>3</sup>CNRS, ERL5294 CRCT, F-31000 Toulouse, France; <sup>4</sup>Laboratoire d'Ingénierie des Systèmes Biologiques et des Procédés, Université de Toulouse, CNRS, INRA, INSA, Toulouse, France; <sup>5</sup>Institut Carnot Lymphome-CALYME, F-31024 Toulouse, France; <sup>6</sup>Laboratoire d'Excellence Toulouse Cancer-TOUCAN, F-31024 Toulouse, France and <sup>7</sup>European Research Initiative on ALK-Related Malignancies, Cambridge, UK

\*CH-A, CQ, AC, NC and FB all contributed equally to this work. §Member of the Equipe Labelisée LIGUE 2017.

©2019 Ferrata Storti Foundation. This is an open-access paper. doi:10.3324/haematol.2018.195131

Received: April 9, 2018.

Accepted: September 21, 2018.

Pre-published: September 27, 2018.

Correspondence: fabienne.meggetto@inserm.fr

---

## Supplemental legends:

**Supplemental Figure 1: Validation of si-ALK transfection and crizotinib treatment in NPM-ALK-positive lymphoma cells.** Protein levels of NPM-ALK and p-NPM-ALK were assessed by western blotting in NPM-ALK(+) KARPAS-299 (KARPAS), COST and SU-DHL1 cells transfected with a siRNA targeting ALK mRNA (si-ALK) or with negative control siRNA (si-CTL) (**A**) or treated or not (PBS) with crizotinib (**B**). The GAPDH protein served as an internal control to ensure equal loading. Results from one representative experiment are shown.

**Supplemental Figure 2: The MIR497 promoter is methylated in NPM-ALK-positive lymphoma cells.** (**A**) Schematic representation of the position of 6 CpG dinucleotides in the promoter region of *MIR497HG*. Percentage of DNA methylation, assessed by bisulfite conversion and pyrosequencing in (**B**) untreated NPM-ALK(+) KARPAS-299 (KARPAS), SU-DHL1, COST cells and in CD4 lymphocytes activated using CD3/CD28 antibodies or (**C**) treated with decitabine. Data represent means  $\pm$  SEM (bars) from 3 independent experiments; \*  $p<0.05$ , \*\*\* $P<0.0001$ , unpaired two-tailed Student's t-test with Welch's correction.

**Supplemental Figure 3: Efficiency of miR-497 mimic transfection in NPM-ALK-positive lymphoma cells.** NPM-ALK(+) COST, SU-DHL1 and KARPAS-299 cells were transfected with negative control miRNA (miR-CTL), mimic miR-497 (miR-497, **A, B, C**) or mimic miR-195 (miR-195, **B**). MiRNA expression was analyzed 72h after transfection by qRT-PCR. SNORD44 served as a relative control. The relative expression levels of miR-195 and miR-497 were expressed as the  $2^{-\Delta\Delta Ct}$  relative to miR-CTL conditions.

**Supplemental Figure 4: NPM-ALK-positive lymphoma cells express CDK4, CDK6 and Rb proteins.** Protein levels of NPM-ALK, p-NPM-ALK, CDK4, CDK6, Rb and GAPDH were assessed by western blotting in NPM-ALK(+) KARPAS-299 (KARPAS), COST and SU-DHL1 cells. The GAPDH protein served as an internal control to ensure equal loading. Results from one representative experiment are shown.

**Supplemental Figure 5: Silencing efficiency of CDK6, CCNE1, CDC25A and E2F3 after siRNA transfection in NPM-ALK-positive lymphoma cells.** NPM-ALK(+) COST, SU-DHL1 and KARPAS-299 (KARPAS) cells were transfected with a siRNA targeting CDK6, CCNE1, CDC25A and E2F3 mRNAs ( si-CDK6, si-CCNE1, si-CDC25A and si-E2F3, respectively) or with negative control siRNA (si-CTL). (**A**) Quantitative RT-PCR analysis of CDK6, CDC25A, CCNE1 and E2F3 mRNA expression. *GAPDH* was used as an internal control and relative mRNAs expression was expressed as the  $2^{-\Delta\Delta Ct}$  relative to si-CTL conditions. (**B**) Protein levels of CDK6, CCNE1, CDC25A and E2F3 were assessed by western blotting in KARPAS-299, COST and SU-DHL1 cells. The GAPDH protein served as an internal control to ensure equal loading. Results from one representative experiment are shown. (**C**) Densitometric analysis was performed using ImageJ software from Wayne Rasband (NIH). Relative protein expression was expressed relative to si-CTL conditions. Data represent means  $\pm$  SEM (bars) from 3 independent experiments. \* $P<0.05$ , \*\* $P<0.001$ , \*\*\* $P<0.0001$  and ns: not significant; unpaired 2-tailed Student's t test with Welch's correction.

**Supplemental Figure 6: CDK6, CCNE1 and E2F3 transfection in NPM-ALK-positive lymphoma cells induce cell cycle alterations.** Cell cycle analysis of NPM-ALK(+) COST and KARPAS-299 (KARPAS) cells transfected with a siRNA targeting E2F3, CDK6 or CCNE1 mRNAs (si-E2F3, si-CDK6 and si-CCNE1 respectively) or with negative control siRNA (si-

CTL). Data represent means  $\pm$  SEM (bars) from 3 independent experiments. \*P<0.05, \*\*\*P<0.0001 and ns: not significant; unpaired 2-tailed Student's t test with Welch's correction.

**Supplemental Figure 7: CDK6, CCNE1 and E2F3 transfection induces apoptosis in NPM-ALK-positive cells.** Assessment of caspase 3/7 activity in NPM-ALK(+) KARPAS-299 (KARPAS) and COST cells transfected with a siRNA targeting CDK6, CCNE1 and or E2F3 mRNAs (si-CDK6, si-CCNE1 and si-E2F3 respectively) or with negative control siRNA (si-CTL). Data represent means  $\pm$  SEM (bars) from 3 independent experiments. \*\*P<0.001; unpaired 2-tailed Student's t test with Welch's correction.

**Supplemental Figure 8: Silencing efficiency of CDK6, CCNE1 and E2F3 after transfection of pool of siRNAs.** Quantitative RT-PCR analysis of CDK6, CCNE1 and E2F3 mRNA expression in NPM-ALK(+) KARPAS-299 (KARPAS) and COST cells transfected with pooled siRNAs targeting CDK6, CCNE1 and E2F3 mRNAs or with negative control siRNA (si-CTL). GAPDH was used as an internal control and relative mRNAs expression was expressed as the  $2^{-\Delta\Delta Ct}$  relative to si-CTL conditions. Data represent means  $\pm$  SEM (bars) from 3 independent experiments. \*P<0.05, \*\*P<0.001, \*\*\*P<0.0001; unpaired 2-tailed Student's t test with Welch's correction.

**Supplemental Figure 9: Ectopic expression of miR-497 induces cell cycle arrest and reduces in vitro growth of NPM-ALK-positive COST and SU-DHL-1 cells.** Cells were transfected with negative control miRNA (miR-CTL) or mimic miR-497 (miR-497). Cells in sub-G1, S and G2M phases of the cell cycle were sorted based on DNA content. Cell cycle distribution was measured 24h post-transfection and showed as a mean of the number of cells in each phase of the cell cycle (sub-G1, S and G2M) of 3 independent experiment (**A**) or as a representative cell cycle distribution for each condition (**B**). \*P < 0.05, \*\*P < 0.001, \*\*\*P < 0.0001 and ns: not significant; using unpaired 2-tailed Student's t test with Welch's correction.

**Supplemental Figure 10: Palbociclib decreased Cdk4/6-specific phosphorylation of Rb protein.** (**A**) Protein levels of Rb and pRb were assessed by Western-blotting in NPM-ALK(+) SU-DHL1, COST and KARPAS-299 (KARPAS) cells treated (1 $\mu$ M) or not (0) with Palbociclib. The GAPDH protein served as an internal control to ensure equal loading. Results from one representative experiment are shown. (**B**) Densitometric analysis was performed using ImageJ software from Wayne Rasband (NIH). Relative protein expression was expressed relative to Rb expression.

**Supplemental Figure 11: Silencing of CDK4 does not reduce cell proliferation in ALK-positive lymphoma cells.** NPM-ALK(+) COST (**A, B and C**), KARPAS-299 (KARPAS) (**D, E and F**) and SU-DHL1 (**G, H and I**) cells were transfected with either an irrelevant siRNA (si-CTL) or a siRNA targeting CDK4. (**C, F and I**) Quantitative RT-PCR analysis of CDK4 mRNA expression in NPM-ALK(+) COST, KARPAS and SU-DHL1 cells transfected with siRNAs targeting CDK4 mRNAs or with negative control siRNA (si-CTL). GAPDH was used as an internal control and relative mRNA expression was expressed as the  $2^{-\Delta\Delta Ct}$  relative to si-CTL conditions. Cell growth (**A, D and G**) and apoptosis (**B, E and H**) were evaluated after si-CDK4 and si-CTL transfection in COST, KARPAS and SU-DHL1 cells. Data represent means  $\pm$  SEM (bars) from 3 independent experiments.

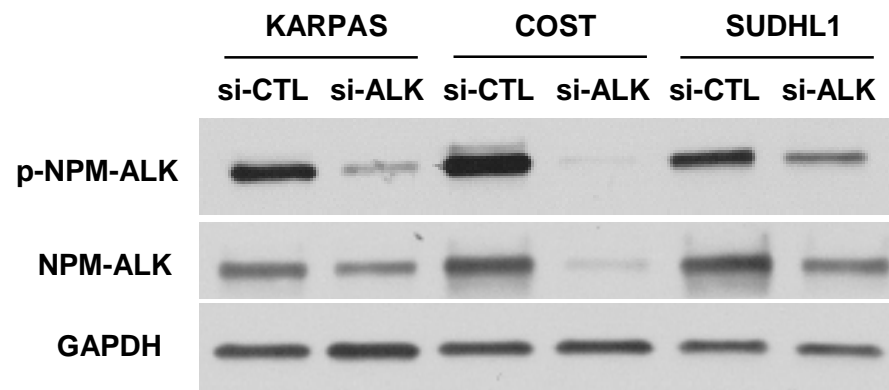
**Supplemental Figure 12: Expression profile of trio genes CCNE1, CDK6 and E2F3 could predict chemotherapy treatment outcome of NPM-ALK(+) pediatric lymphomas (**A**)** Quantitative RT-PCR analysis of CDK6, CCNE1 and E2F3 mRNA expression in NPM-ALK(+) cells.

lymphoma patients (n=55). Data were normalized against equivalent mRNA levels from reactive lymph node tissue samples (RLN; n=12). Data represent means  $\pm$  SEM (bars), \*\*\*P<0.0001; unpaired 2-tailed Student's t test with Welch's correction. (B) ROC (Receiver Operating Characteristics) curve obtained from CCNE1, CDK6, E2F3 genes-based score from NPM-ALK(+) ALCL samples (n=44) for whose event free survival is known; Cut-off value (-0.038) and AUC (Area under curve; 0.65) were calculated. Kaplan-Meier survival curves stratified by event free survival (cut-off obtained with ROC curve) (C) the patients (D) including the NPM-ALK(+) pediatric ALCL patients. (E) Box-plot distributions of the gene score in "relapsing" after chemotherapy cure (grey, n=23) and "non-relapsing" (white, n=19) groups in NPM-ALK(+) pediatric lymphomas. \*P<0.05; unpaired 2-tailed Student's t test".

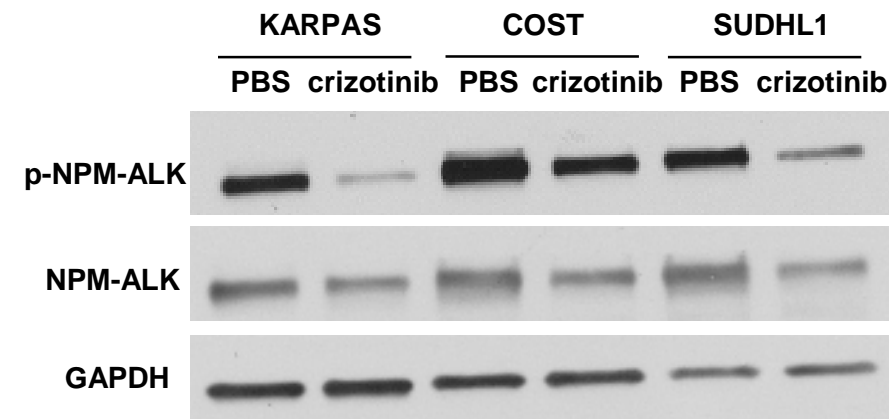
**Supplemental Table 1:** Sequences of siRNAs and primers used for quantitative real-time PCR and pyrosequencing analysis.

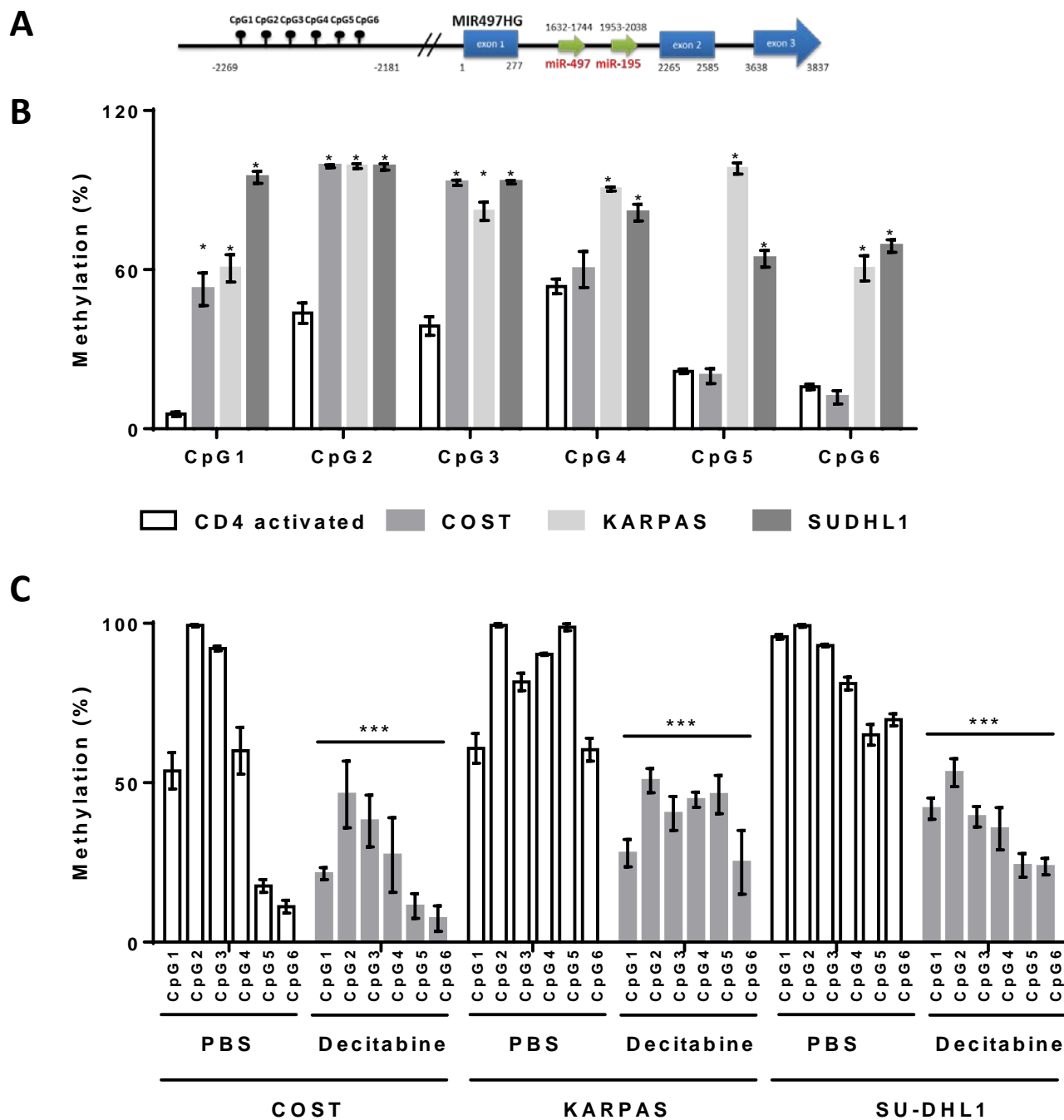
**Supplemental Table 2: MiRNAs with differential expression in NPM-ALK(+) ALCL lymph node primary tissues sorted according to fold change in expression (adapted from Congras et al, <sup>22</sup>).**

A

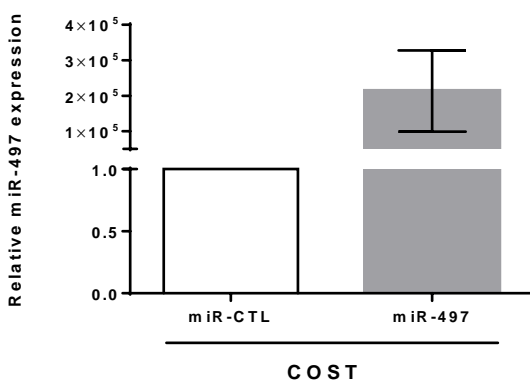


B

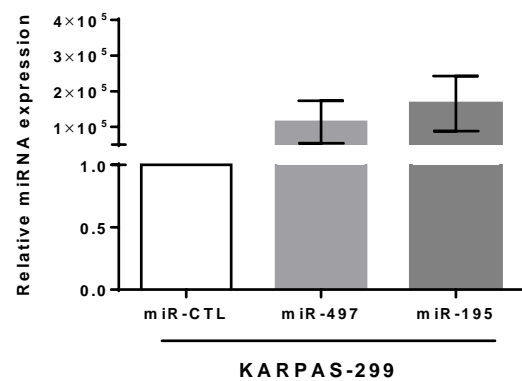




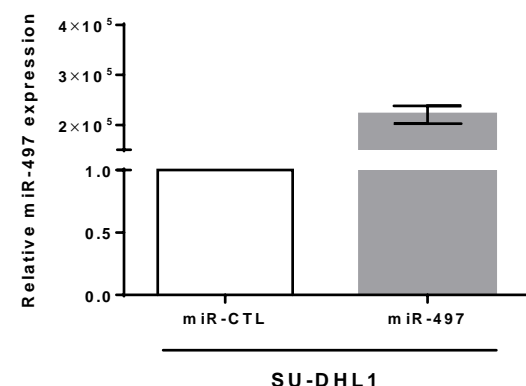
A

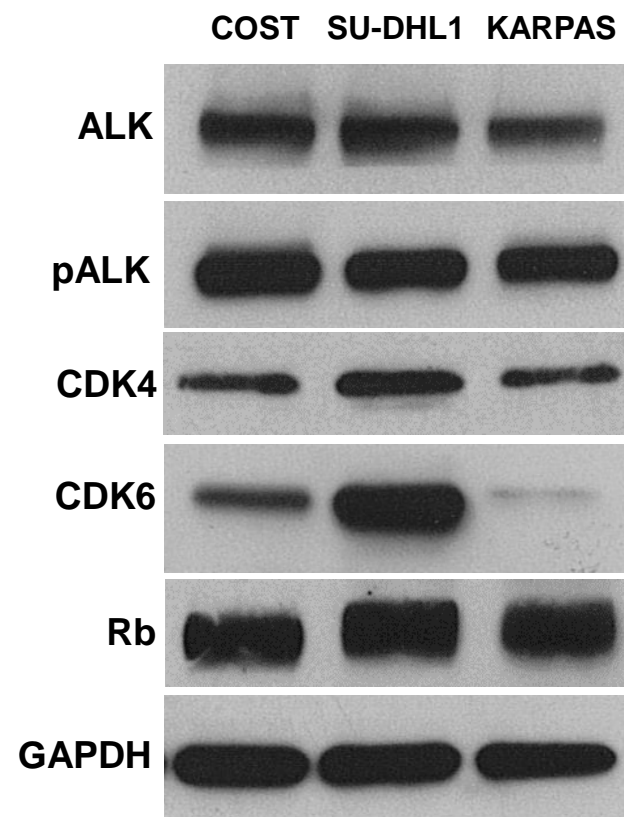


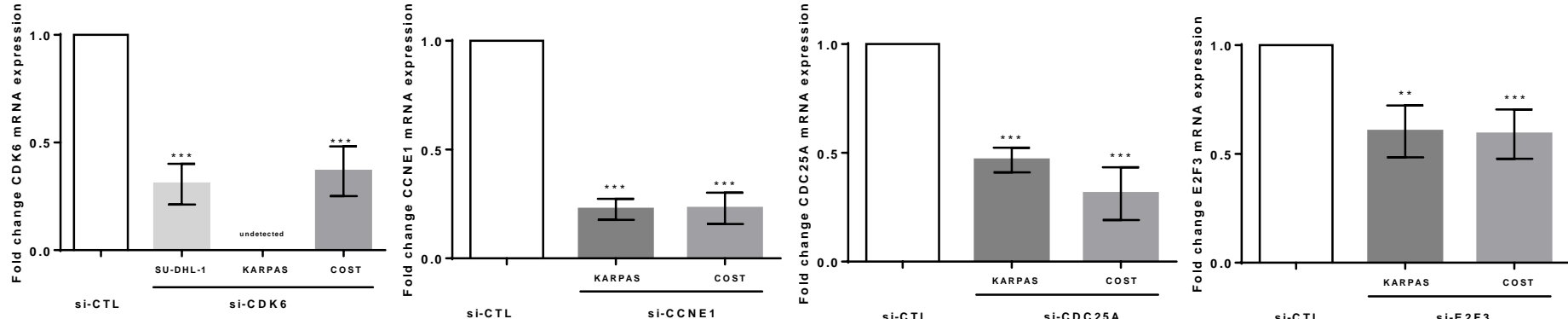
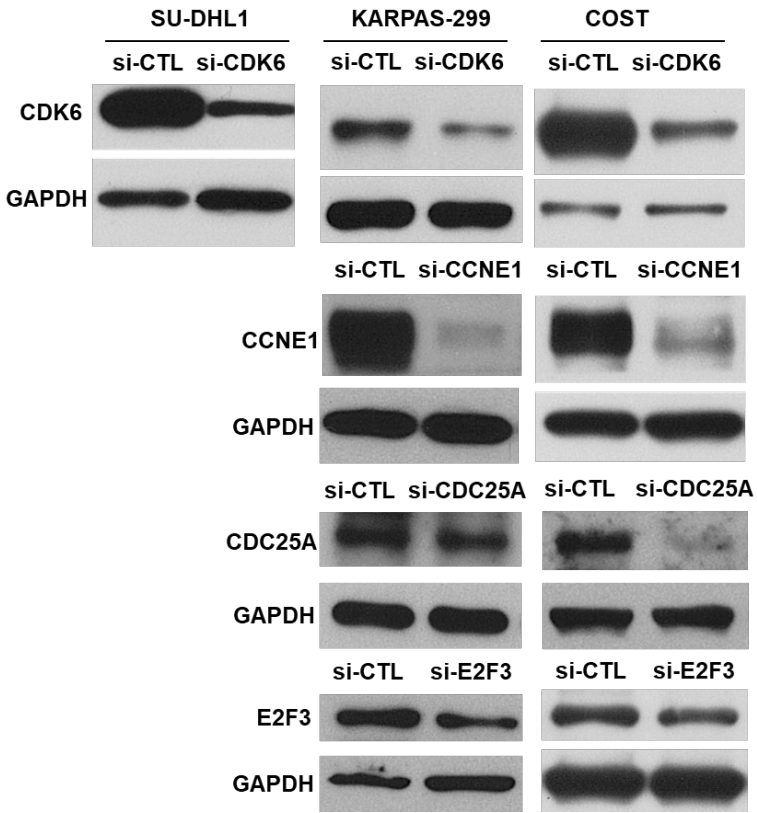
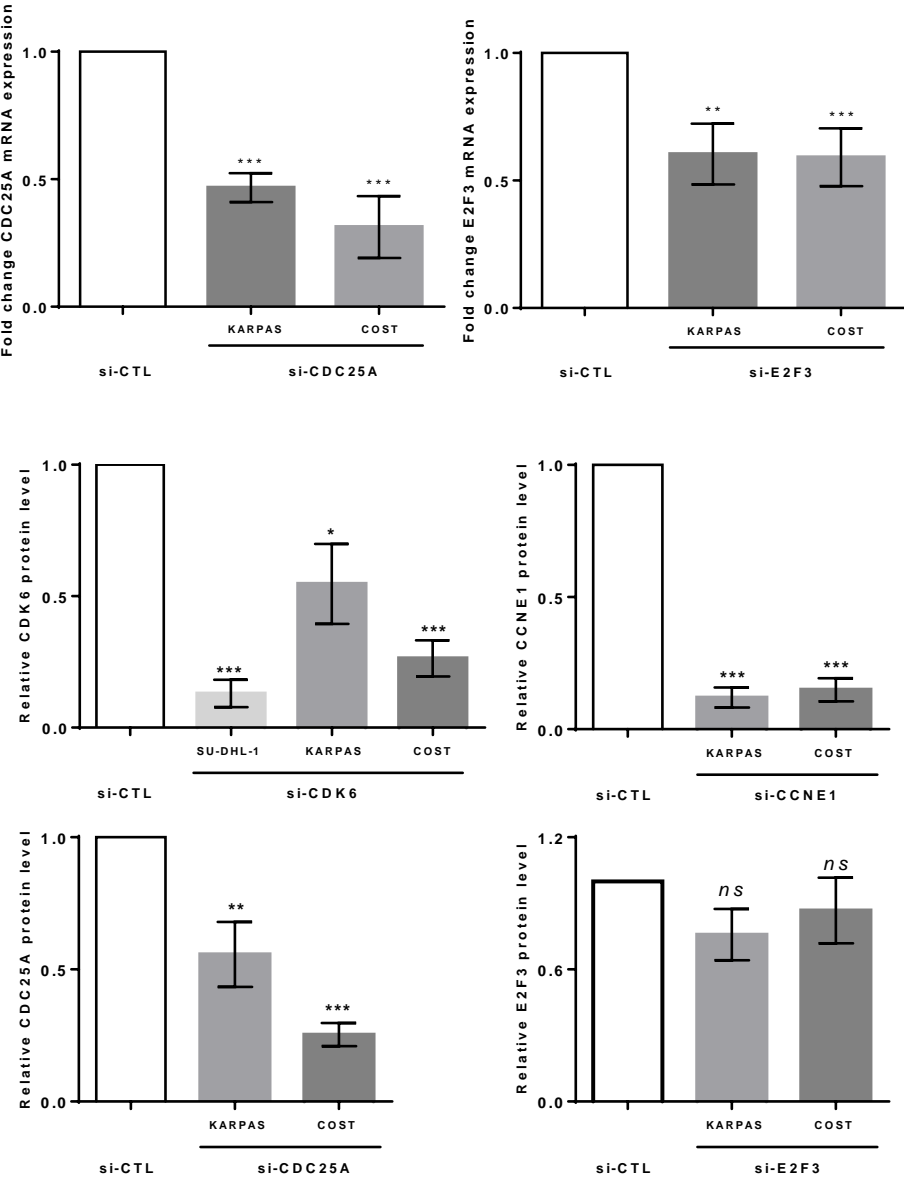
B

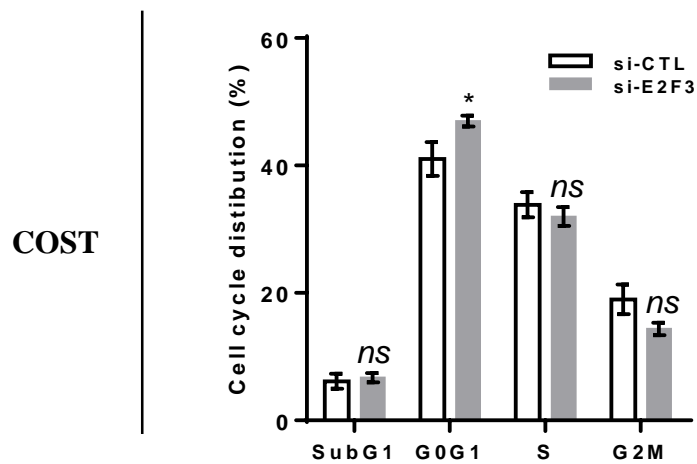
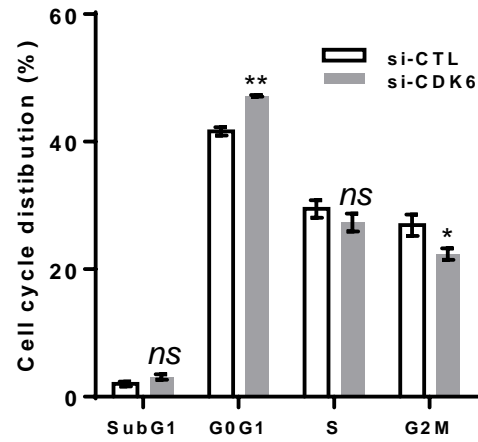
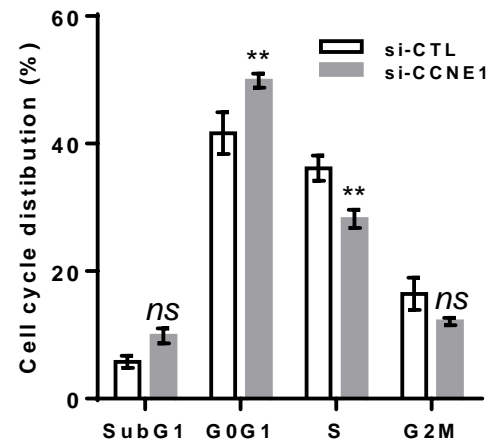
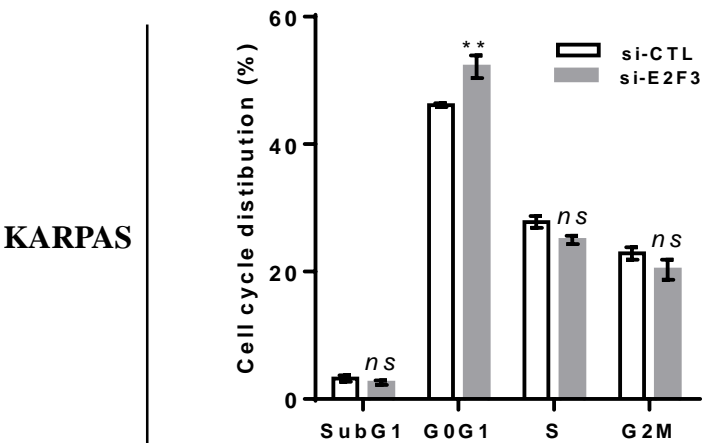
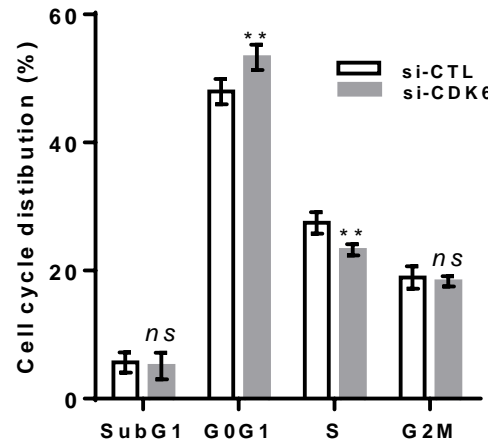
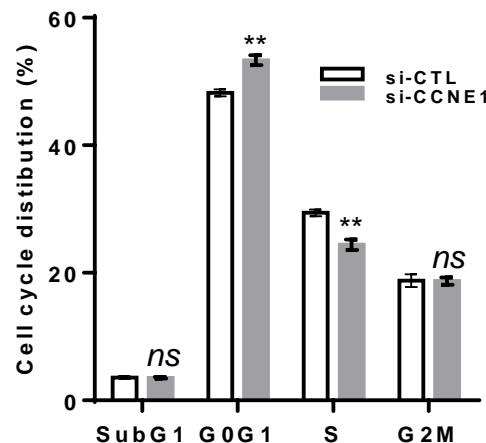


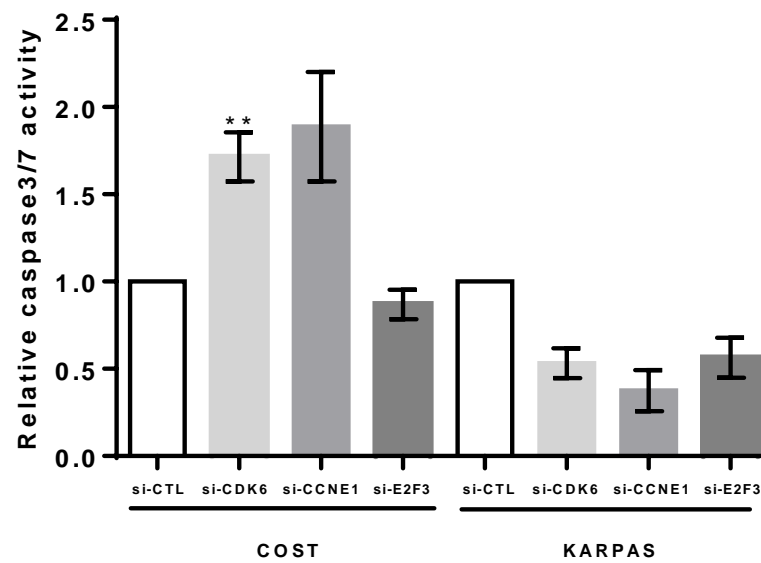
C

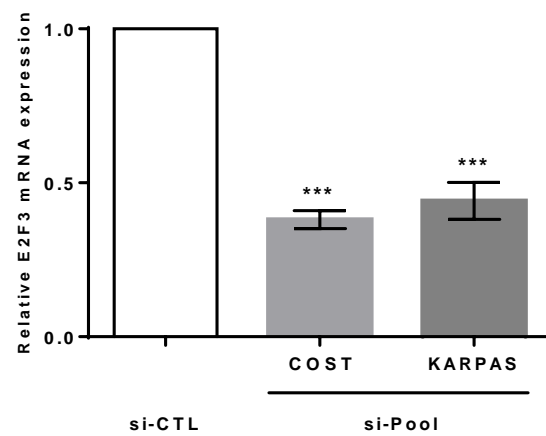
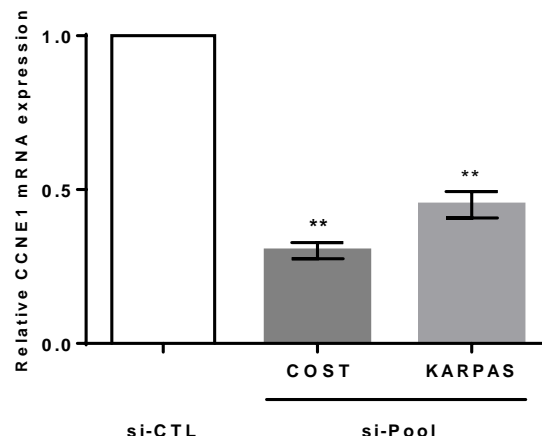
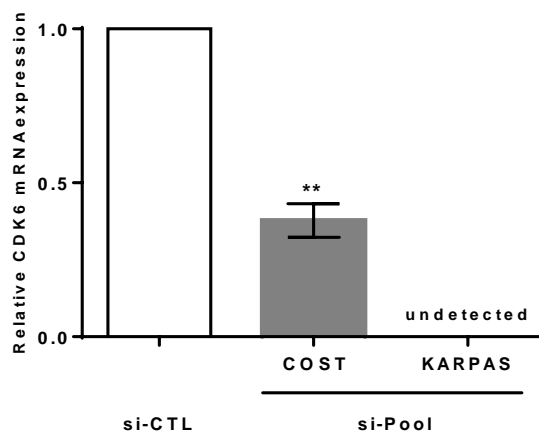


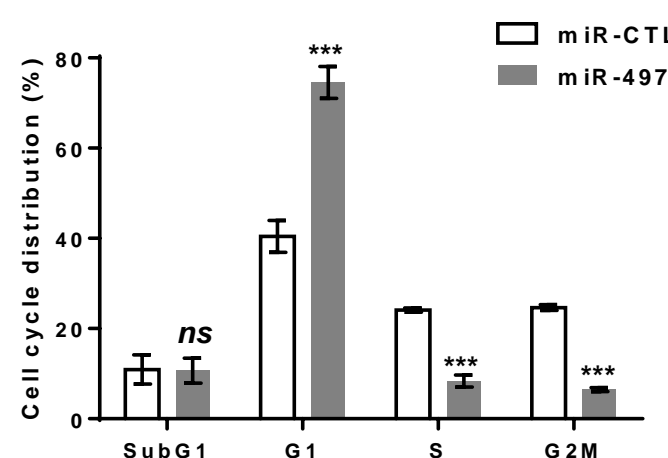
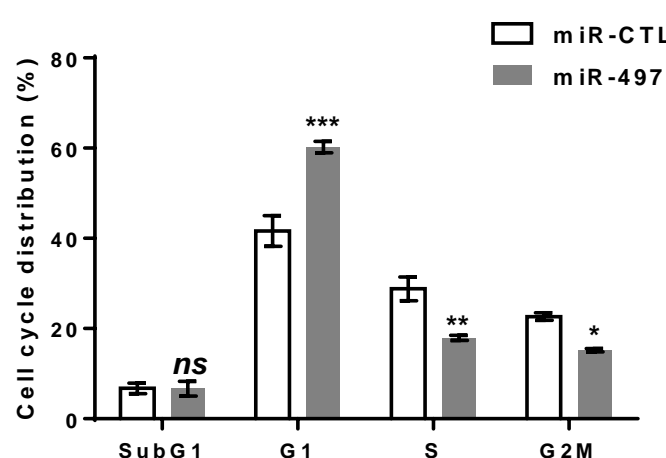
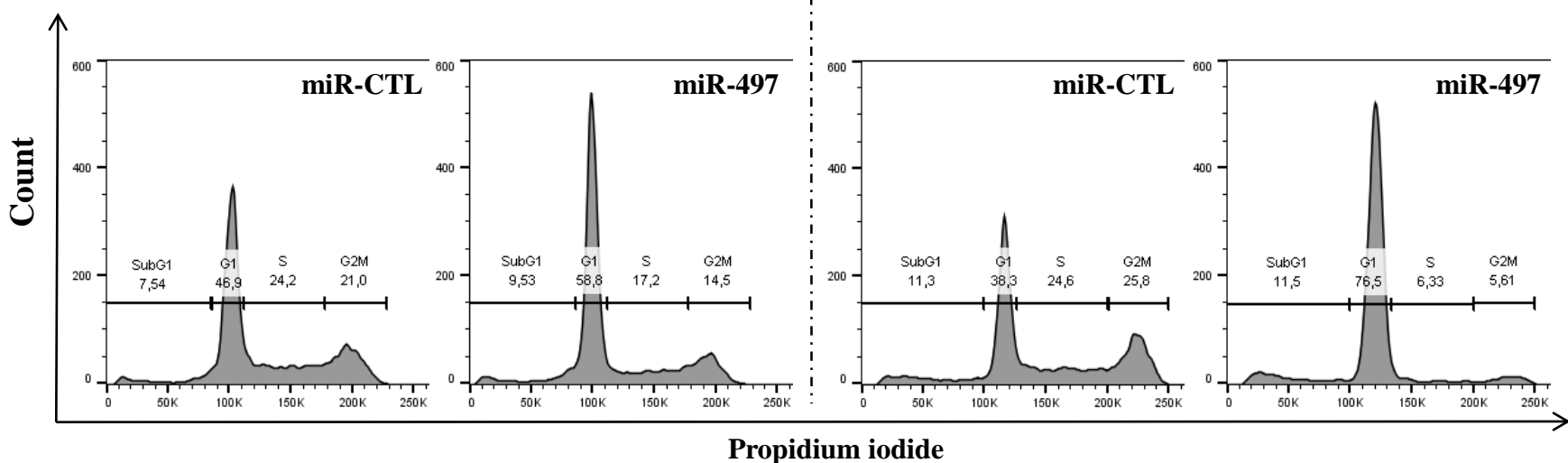


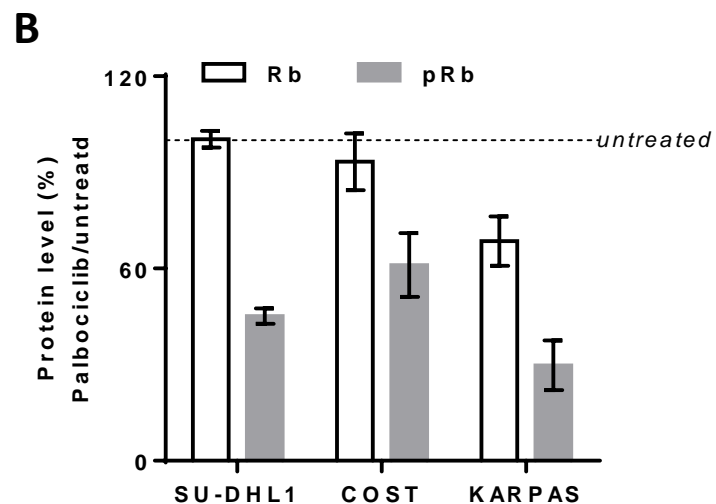
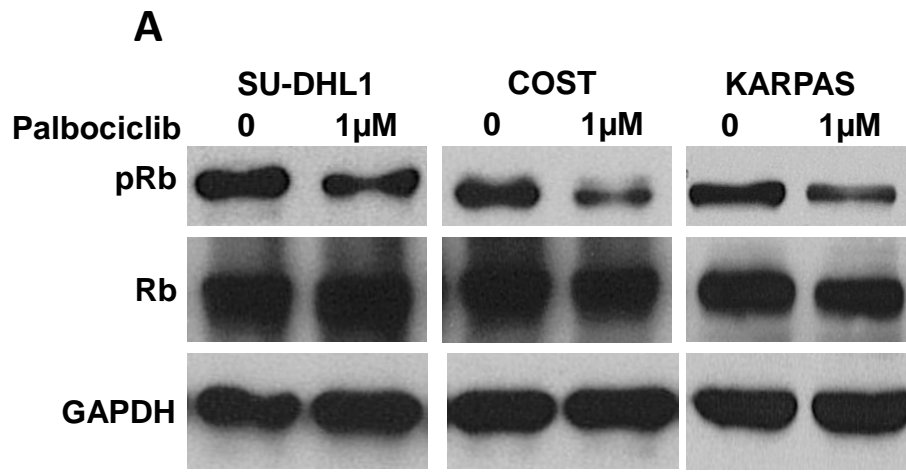
**A****B****C**

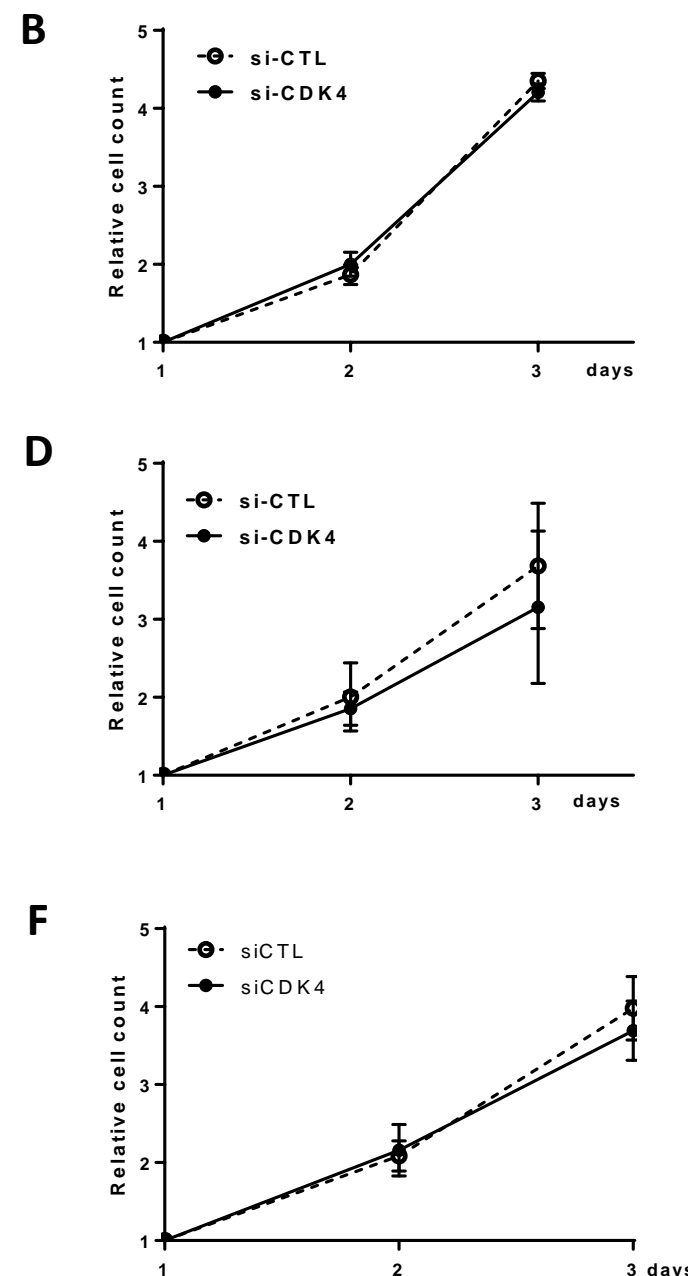
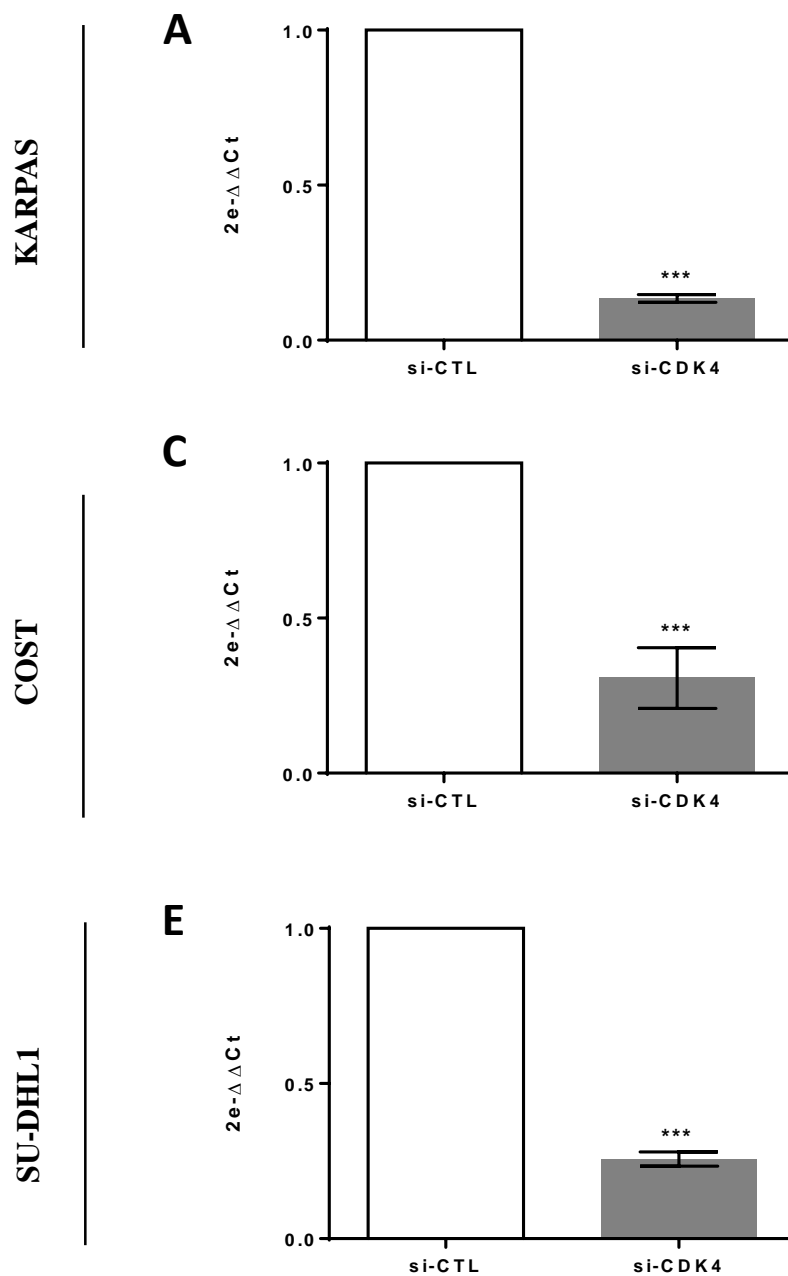
**A****B****C****D****E****F**

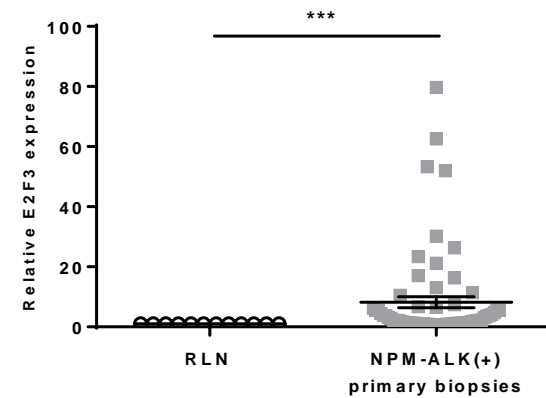
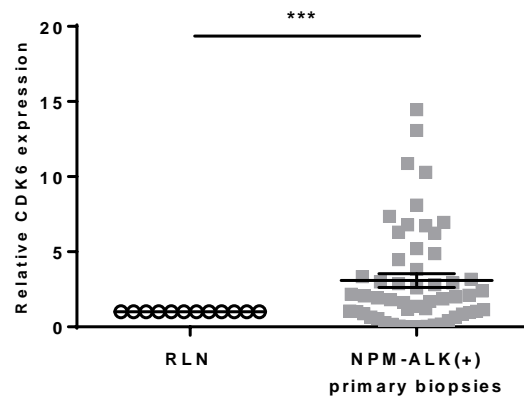
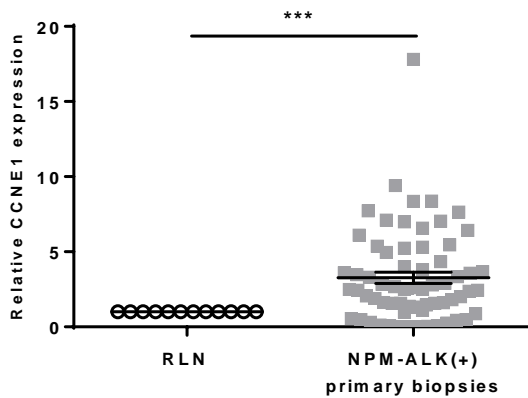
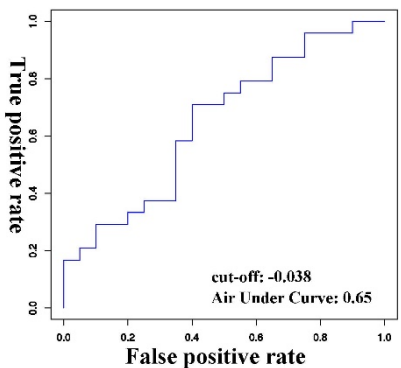
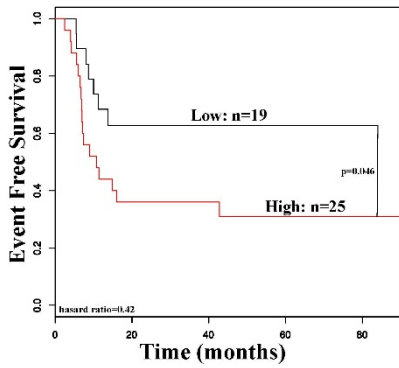
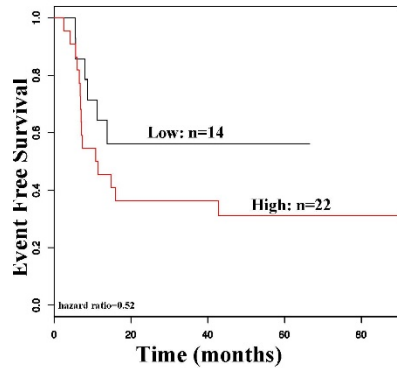
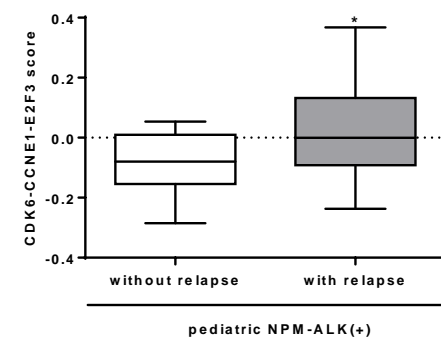




**COST****SU-DHL1****A****B**





**A****B****C****D****E**

<b>qRT-PCR primers</b>	
<b>CDC25A-foward</b>	CTGTCGCCTGTCACCAACCTG
<b>CDC25A-reverse</b>	TCGGAGGAGCCCATTCTCTGC
<b>CDK6-foward</b>	CCCCAGAGTCTGATTACCTGC
<b>CDK6-reverse</b>	ACATAGCCTCTGCCAAGC
<b>CCNE1-foward</b>	GGTTTCAGGGTATCAGTGGTGCG
<b>CCNE1-reverse</b>	TCTGTGGGTCTGTATGTTGTGTC
<b>E2F3-foward</b>	GCACTACGAAGTCCAGATAGTCC
<b>E2F3-reverse</b>	GGCTCAGGAGCTGAATGAA
<b>CCND3-foward</b>	CTGGATCGCTACCTGTCTTG
<b>CCND3-reverse</b>	TCCCACTTGAGCTTCCCTAG
<b>GAPDH-foward</b>	CGGGAAGCTTGTGATCAATGG
<b>GAPDH-reverse</b>	GGCAGTGATGGCATGGACTG
<b>MLN51-foward</b>	TAATCCCAGTTACCCTTATGCTCCA
<b>MLN51-reverse</b>	GTTATAGTAGGTCACTCCTCCATATAACCTGT
<b>siRNA</b>	
<b>CDC25A siRNA</b>	CUGUGAUUUUGAUAGCUUU
<b>CDK6 siRNA</b>	UUCUACGAAACAUUUCUGC
<b>CCNE1 siRNA</b>	GAGCUGUUUCUGAGGAGCC
<b>E2F3 siRNA</b>	AAACCGCGGUAGAUACGUCUC
<b>STAT3 siRNA</b>	AACAUUCUGCCUAGAACGGCUA
si-CTL	Smart Pool 4609 (Dharmacon)
<b>bisulfite sequencing primers</b>	
<b>MiR-497-F</b>	TGTTTTTAGGAGGGATTAGG
<b>MiR-497-Rb</b>	[Btn]TCACCTCCAAAACATCTAAATAACAATAT
<b>MiR-497-sequence</b>	TTTAGGTTGGGGTTTTA

Downregulated miRNAs in human	Total	miRNA names
<b>NPM-ALK(+) and NPM-ALK(-) ALCL lymph node primary tissues ††</b>	24	let-7a, let-7c, let-7g, miR-1201, miR-1256, miR-126, miR-140-3p, miR-150, miR-151-5p, miR-204, miR-26a, miR-29a, miR-29c, miR-30b, miR-342-3p, miR-342-5p, miR-361-3p, miR-361-p, miR-374a*, miR-384, miR-548, miR-655, miR-99a
<b>NPM-ALK(+) ALCL lymph node primary tissues ††</b>	39	let-7b, let-7d, miR-100, miR-10b, miR-1179, miR-122, miR-1259, miR-125b, miR-1277, miR-1279, miR-1324, miR-139-3p, miR-139-5p, miR-145, miR-155, miR-15b, miR-190b, <u>miR-195</u> , miR-19a*, miR-26b, miR-30a, miR-30a*, miR-30d, miR-31, miR-449a, <u>miR-497</u> , miR-508-5p, miR-509-3p, miR-514, miR-545*, miR-548g, miR-561, miR-590-3p, miR-599, miR-603, miR-606, miR-609, miR-769-5p, miR-802
<b>NPM-ALK(-) ALCL lymph node primary tissue ††</b>	8	let-7e, miR-194, miR-199a-3p, miR-26a-1*, miR-26a-2*, miR-335, miR-499-5p, miR-633

Normalized against equivalent miRNA levels from normal reactive lymph node (n=3)

adaptated from Congras et al,<sup>22</sup>